RSC Advances

PAPER

View Article Online
View Journal | View Issue

Check for updates

Cite this: *RSC Adv.*, 2018, **8**, 18656

Ionic dynamics of the cation in organic–inorganic hybrid compound $(CH_3NH_3)_2MCl_4$ (M = Cu and Zn) by ^{1}H MAS NMR, ^{13}C CP MAS NMR, and ^{14}N NMR

Ae Ran Lim *[ab]

Received 18th March 2018
Accepted 15th May 2018

DOI: 10.1039/c8ra02363h

rsc.li/rsc-advances

The ionic dynamics of $(CH_3NH_3)_2MCl_4$ (M = Cu, Zn) by ^{1}H magic-angle spinning (MAS) nuclear magnetic resonance (NMR), ^{13}C cross-polarization (CP) MAS NMR, and ^{14}N NMR are investigated as a function of temperature with a focus on the role of the $CH_3NH_3^+$ cation. The molecular motions in $(CH_3NH_3)_2MCl_4$ are also discussed based on the ^{1}H spin–lattice relaxation time in the rotating coordinate frame $T_{1\rho}$. From the ^{1}H $T_{1\rho}$ results, the activation energies for the tumbling motion of ^{1}H for CH_3 and NH_3 were similar, and the uniaxial rotations occurred within a large temperature range. The molecular motions for ^{13}C and ^{14}N of the main chain in the $CH_3NH_3^+$ cation were rigid, whereas those for ^{1}H of the side chain in the $CH_3NH_3^+$ cation were very free at high temperatures. $T_{1\rho}$ provides insight into the changes in the cation reorientation rates induced by heating at high temperatures.

Open Access Article. Published on 22 May 2018. Downloaded on 4/5/2026 12:25:35 AM.
This article is licensed under a Creative Commons Attribution 3.0 Unported Licence.

1. Introduction

Hybrid organic–inorganic compounds have been known since 1976 but recently they have been revisited due to their potential use as substitute materials for perovskites.[1–6] Metal complexes with the formula $(CH_3NH_3)_2MCl_4$ (M = Mn, Fe, Cu, Zn, Cd) can be classified into two groups from a crystal structure point of view.[7–14] One group $(CH_3NH_3)_2MCl_4$ (M = Mn, Fe, Cd) has a perovskite-type layer structure consisting of cationic layers and layers of corner-sharing chlorine octahedra with a divalent metal ion at the center.[15–18] These compounds are characterized by a two-dimensional metal–chlorine network widely separated from one another by methyl ammonium groups. The metal ions are surrounded by a slightly distorted chlorine octahedron, Cl_6. The other group, to which $(CH_3NH_3)_2MCl_4$ (M = Cu, Zn) belongs, consists of discrete $CH_3NH_3^+$ and MCl_4^{2-} ions packed in an arrangement similar to orthorhombic K_2SO_4-like members.[19,20] In these crystals, unassociated Cl_4 tetrahedra are presented instead of corner-sharing layers of chlorine octahedra. Hydrogen-bonding takes place between the hydrogens of $CH_3NH_3^+$ and Cl^-, and the several different possible hydrogen-bond configurations can give rise to structural phase transitions.

The $(CH_3NH_3)_2CuCl_4$ compound with M = Cu undergoes a structural phase transition at 348 K (= T_C), with the respective phases denoted as orthorhombic structure at high temperature and monoclinic structure at room temperature.[21] A sharp peak at 230 K from a thermal capacity experiment was also reported by White and Staveley.[22] In the case of $(CH_3NH_3)_2ZnCl_4$ with M = Zn, the existence of a phase transition at 483 K (= T_C) was reported by calorimetric, dielectric, thermal expansion, and optical measurements.[23] However, a transition at 426 K (= T_C') was reported from Raman and IR spectra but not by differential scanning calorimetry (DSC), differential thermal analysis (DTA), and ^{1}H nuclear magnetic resonance (NMR) measurements. The structure of $(CH_3NH_3)_2ZnCl_4$ is orthorhombic at high temperatures and monoclinic at low temperatures. In addition, it has been reported from low-temperature DSC that a phase transition exists at 265 K during heating.[24,25]

Following previous NMR investigations, the spin–lattice relaxation time T_1 of ^{1}H in the CH_3 and NH_3 groups of $(CH_3NH_3)_2CuCl_4$ at the Larmor frequencies of 12 and 26 MHz was reported. The spectra of the two groups overlap at high temperatures and separate at low temperatures.[25] The T_1 at low temperatures exhibits a strong temperature dependence. Moreover, the self-diffusion and reorientation of the methylammonium ions in $(CH_3NH_3)_2ZnCl_4$ was reported by ^{1}H NMR.[26] In addition, the spin–spin relaxation time T_2 of ^{63}Cu and ^{35}Cl in $(CH_3NH_3)_2CuCl_4$ has been reported at 1.75 K.[27,28] In the case of $(CH_3NH_3)_2ZnCl_4$, ^{1}H T_1 NMR studies at the Larmor frequency of 20 MHz revealed that the cation in the highest-temperature phase performs isotropic rotation and self-diffusion. The cation in the low-temperature phase undergoes reorientation about its C–N bond axis.[29] Although the structural phase transitions in $(CH_3NH_3)_2CuCl_4$ and $(CH_3NH_3)_2ZnCl_4$ have been performed by several research groups, the corresponding molecular motions and structural geometry changes have not been fully studied by NMR in the rotating frame.

[a]*Analytical Laboratory of Advanced Ferroelectric Crystals, Jeonju University, Jeonju 55069, Korea . E-mail: aeranlim@hanmail.net; arlim@jj.ac.kr; Fax: +82-063-220-2053; Tel: +82-063-220-2514*

[b]*Department of Science Education, Jeonju University, Jeonju 55069, Korea*

This journal is © The Royal Society of Chemistry 2018

Open Access Article. Published on 22 May 2018. Downloaded on 4/5/2026 12:25:35 AM.
This article is licensed under a Creative Commons Attribution 3.0 Unported Licence.

In the present study, to clarify the ionic dynamics of $CH_3NH_3^+$ cations and to also obtain information of the mechanism of the phase transition in $(CH_3NH_3)_2MCl_4$ (M = Cu, Zn), the chemical shifts and spin–lattice relaxation time in the rotating coordinate frame $T_{1\rho}$ were measured as a function of temperature using ^{1}H magic-angle spinning (MAS) NMR and ^{13}C cross-polarization (CP) MAS NMR. In addition, the ^{14}N NMR spectra in $(CH_3NH_3)_2ZnCl_4$ single crystals in the laboratory frame were discussed in order to elucidate the structural geometry. We focus on the structural phase transitions of compounds with the formula $(CH_3NH_3)_2MCl_4$. We use these results to analyze the behavior of CH_3 and NH_3 near the phase transition temperature from the results of ^{1}H MAS NMR, ^{13}C CP MAS NMR, and ^{14}N NMR. In addition, we compare the structural geometries of $(CH_3NH_3)_2MCl_4$ (M = Cu, Zn) obtained here and $(CH_3NH_3)_2MCl_4$ (M = Mn, Cd) previously reported.

2. Materials and methods

2.1. Crystal structure

The $(CH_3NH_3)_2CuCl_4$ undergoes a phase transition at 348 K. At temperatures below $T_C = 348$ K, the structure is monoclinic, the space group is $P2_1/c$, and the lattice constants are $a = 7.155$ Å, $b = 7.424$ Å, $c = 9.814$ Å, and $\beta = 109.18°$.[6] The crystal structure at 363 K is orthorhombic, the space group is *Ccmb*, and the lattice constants are $a = 7.34$ Å, $b = 18.71$ Å, and $c = 7.33$ Å.[30,31] The monoclinic structure at room temperature is shown in Fig. 1.[3] Here, the methylammonium moieties are located between the layers and are connected by hydrogen bonds to the Cl^- ions. Further, $(CH_3NH_3)_2ZnCl_4$ undergoes a phase transition at 483 K. At room temperature, the crystal is monoclinic with the space group $P2_1/c$, and the lattice constants are $a = 10.873$ Å, $b = 12.655$ Å, $c = 7.648$ Å, $\beta = 96.71°$, and $Z = 4$.[19,23,26,32] Here, the two inequivalent sites, $CH_3(1)$ and $CH_3(2)$, and $NH_3(1)$ and $NH_3(2)$, in $(CH_3NH_3)_2ZnCl_4$ were reported by Morosin *et al.*[19]

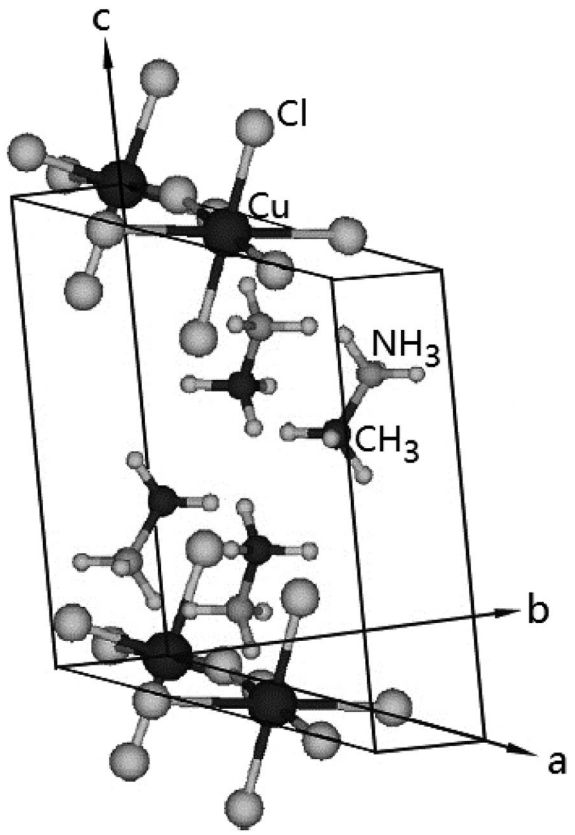

Fig. 1 The structure of $(CH_3NH_3)_2CuCl_4$ at room temperature.

2.2. Experimental method

Single crystals of $(CH_3NH_3)_2MCl_4$ (M = Cu, Zn) were prepared by the slow evaporation of an aqueous solution of stoichiometric amounts of $CH_3NH_3{\cdot}HCl$ and MCl_2 (M = Cu, Zn) at room temperature. The color of $(CH_3NH_3)_2CuCl_4$ single crystals is brown with flat parallelepipeds. In addition, $(CH_3NH_3)_2ZnCl_4$ single crystals are colorless and transparent with a square shape. The phase transition temperatures were determined using DSC (Dupont, 2010) measurements at a heating rate of 10 K min^{-1}.

^{1}H MAS NMR and ^{13}C CP MAS NMR spectra of $(CH_3NH_3)_2MCl_4$ (M = Cu, Zn) in the rotating coordinate frame were obtained at the Larmor frequencies of $\omega_0/2\pi = 400.13$ and 100.61 MHz, respectively, using a Bruker 400 MHz NMR spectrometer at the Korea Basic Science Institute, Western Seoul Center. Powdered samples were placed in a 4 mm CP MAS probe, and the MAS rate was set to 10 kHz for both ^{1}H MAS and ^{13}C CP MAS measurements to minimize the spinning sideband overlap. The chemical shifts were referred with respect to tetramethylsilane (TMS). The spin–lattice relaxation times for ^{1}H and ^{13}C of $(CH_3NH_3)_2MCl_4$ in the rotating coordinate frame were determined using a $\pi/2 - t$ sequence by varying the duration of the spin-locking pulses. In the case of $(CH_3NH_3)_2CuCl_4$, the width of the $\pi/2$ pulse used for measuring the $T_{1\rho}$ values of ^{1}H and ^{13}C was 3.9 μs, with a spin-locking field of 64.1 kHz. In the case of $(CH_3NH_3)_2ZnCl_4$, the width of the $\pi/2$ pulse used for measuring the $T_{1\rho}$ values of ^{1}H and ^{13}C was 4.5 and 5.6 μs, with the spin-locking field of 55.55 kHz and 44.64 kHz, respectively. The power level for ^{1}H and ^{13}C was 4 db and 6.5 db, respectively. The ^{13}C $T_{1\rho}$ values were measured by varying the duration of the ^{13}C spin-locking pulse applied after the CP preparation period.

In addition, the ^{14}N NMR spectra of the $(CH_3NH_3)_2ZnCl_4$ single crystals in the laboratory frame were measured using a Unity INOVA 600 NMR spectrometer at the same facility. The static magnetic field was 14.1 T and the Larmor frequency was set to $\omega_0/2\pi = 43.342$ MHz. The ^{14}N NMR experiments were conducted using a solid-echo pulse sequence.

Temperature-dependent NMR spectra were recorded at 180–430 K as the chemical shift and relaxation time could not be determined outside this temperature range, because of the limitations of the spectrometer used. The sample temperatures were maintained within ±0.5 K by controlling the nitrogen gas flow and heater current.

3. Results and discussion

The DSC analysis in $(CH_3NH_3)_2CuCl_4$ revealed two endothermic peaks at 347 K (= T_C) and 517 K (= T_m) related to the phase

Open Access Article. Published on 22 May 2018. Downloaded on 4/5/2026 12:25:35 AM.
This article is licensed under a Creative Commons Attribution 3.0 Unported Licence.

transition and melting point, respectively, as shown in Fig. 2. The enlarged peak near 347 K in Fig. 2 is very small relative to the other endothermic peak. In the case of $(CH_3NH_3)_2ZnCl_4$, two endothermic peaks are obtained at 475 K ($= T_C$) and 525 K ($= T_m$), which are due to the phase transition and melting point. In order to understand the additional endothermic peaks at high temperature, we conduct optical polarizing microscopy. The peaks of 517 and 525 K in $(CH_3NH_3)_2CuCl_4$ and $(CH_3NH_3)_2ZnCl_4$, respectively, are not related to physical changes such as structural phase transitions; they are instead related to the melting point. The phase transition temperatures obtained here are consistent with previous results.[21,23] This suggests that the differences in the chemical properties of Cu and Zn are responsible for the variations of the phase transition temperatures T_C in the two crystals.

The NMR spectra for ^1H in $(CH_3NH_3)_2MCl_4$ (M = Cu, Zn) were recorded by MAS NMR at a frequency of 400.13 MHz. In the case of the two compounds, the spectrum of the two peaks is assigned to the ^1H in CH_3 and NH_3. One of them, the spectrum of the two peaks at chemical shifts of $\delta = 3.82$ and 12.52 in $(CH_3NH_3)_2CuCl_4$ at room temperature, is presented in Fig. 3. Here, the unit of the NMR scale is represented according to the IUPAC convention.[33,34] The spinning sidebands for CH_3 are marked with open circles and those for NH_3 are marked with crosses. The line component of the lower chemical shift is attributed to the ^1H in CH_3, and that of the higher chemical shift is attributed to the ^1H in NH_3. The protons of CH_3 and NH_3 are distinguished from the ^1H chemical shifts. In the case of $(CH_3NH_3)_2CuCl_4$ across the phase transition temperature of T_C, the chemical shift slowly and monotonously decreases with temperature, indicating that the environments of the surrounding ^1H in the CH_3 and NH_3 groups change continuously (see Fig. 4(a)). However, the proton spectrum of the two peaks in $(CH_3NH_3)_2ZnCl_4$ at room temperature is recorded at chemical shifts of $\delta = 2.88$ and 6.75. The ^1H chemical shifts in

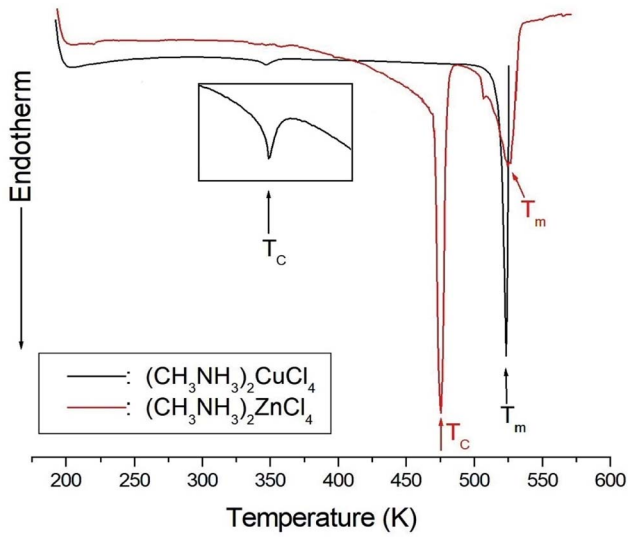

Fig. 2 Differential scanning calorimetry thermogram of $(CH_3NH_3)_2CuCl_4$ and $(CH_3NH_3)_2ZnCl_4$ single crystals.

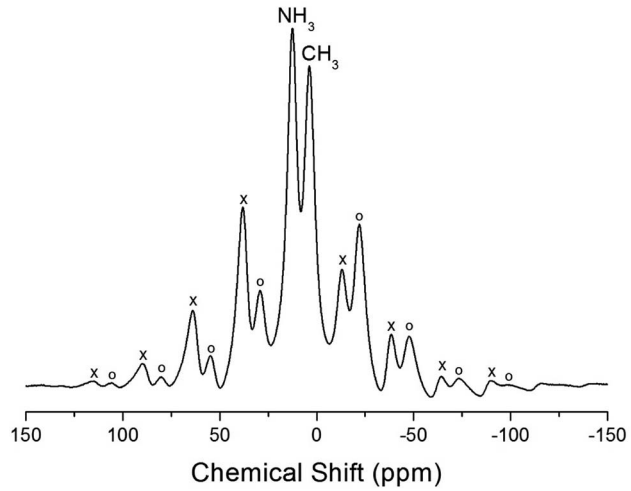

Fig. 3 ^1H MAS NMR spectra of $(CH_3NH_3)_2CuCl_4$ at 300 K (the spinning sidebands are marked with crosses and open circles).

$(CH_3NH_3)_2ZnCl_4$ are almost constant with temperature, as shown in Fig. 4(b).

The ^1H spin–lattice relaxation times in the rotating coordinate frame of $(CH_3NH_3)_2MCl_4$ (M = Cu, Zn) were obtained for the CH_3 and NH_3 at several temperatures. The nuclear magnetization decay of ^1H follows a single exponential function. Thus, $T_{1\rho}$ can be determined by fitting the traces with the following equation:[35]

$$S(t)/S(\infty) = \exp(-t/T_{1\rho}), \quad (1)$$

where $S(t)$ is the magnetization with the spin-locking pulse duration t and $S(\infty)$ is the total nuclear magnetization of ^1H at thermal equilibrium. The values of ^1H $T_{1\rho}$ for two compounds in the rotating coordinate frame between 180 and 430 K are shown in Fig. 5(a) and (b) as a function of the inverse temperature. The $T_{1\rho}$ values for the methyl protons and ammonium protons in the $CH_3NH_3^+$ cations exhibit similar trends with temperature. The $T_{1\rho}$ values of ^1H in the CH_3 and NH_3 groups of $(CH_3NH_3)_2CuCl_4$ are almost continuous near T_C, and these values are of the order of milliseconds. Above 400 K, the two $T_{1\rho}$ values abruptly decrease, and the ^1H $T_{1\rho}$ values for CH_3 are longer than those for NH_3. In contrast, the significant change in the ^{13}C $T_{1\rho}$ values of $(CH_3NH_3)_2ZnCl_4$ is strongly affected, which is primarily considered the result of molecular motions. Further, the variation of $T_{1\rho}$ with temperature exhibits a minimum of 16.3 and 12.8 ms for CH_3 and NH_3 near 400 K, respectively. This behavior of $T_{1\rho}$ indicates that distinct molecular motions are present. It is clear that the minimum $T_{1\rho}$ is attributable to the uniaxial rotation of CH_3 and NH_3 ions. The experimental value of $T_{1\rho}$ is expressed in terms of the isotropic correlation time τ_C for molecular motion using the Bloembergen–Purcell–Pound (BPP) theory,[36] according to which the $T_{1\rho}$ value for a spin–lattice interaction of molecular motion is given by[37–39]

$$(nT_{1\rho}^{-1}) = 0.05(\mu_o/4\pi)^2 (\gamma_H\gamma_C\hbar/r_{H-C}^3)^2 [4a + b + 3c + 6d + 6e], \quad (2)$$

This journal is © The Royal Society of Chemistry 2018

Open Access Article. Published on 22 May 2018. Downloaded on 4/5/2026 12:25:35 AM.
This article is licensed under a Creative Commons Attribution 3.0 Unported Licence.

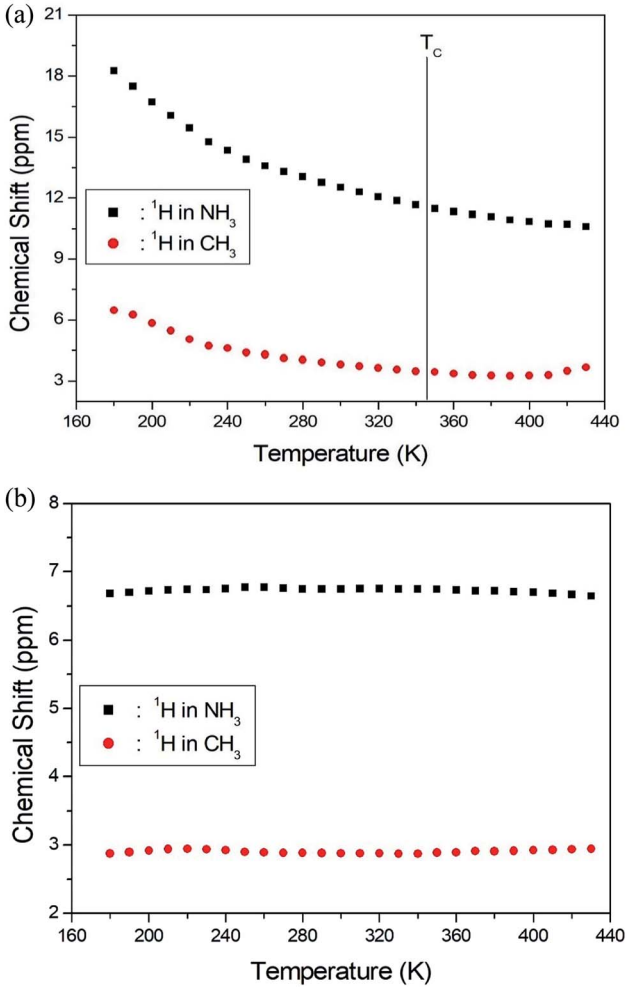

Fig. 4 (a) ^{1}H chemical shifts for CH_3 and NH_3 groups in $(CH_3NH_3)_2CuCl_4$ as a function of temperature. (b) ^{1}H chemical shifts for CH_3 and NH_3 groups in $(CH_3NH_3)_2ZnCl_4$ as a function of temperature.

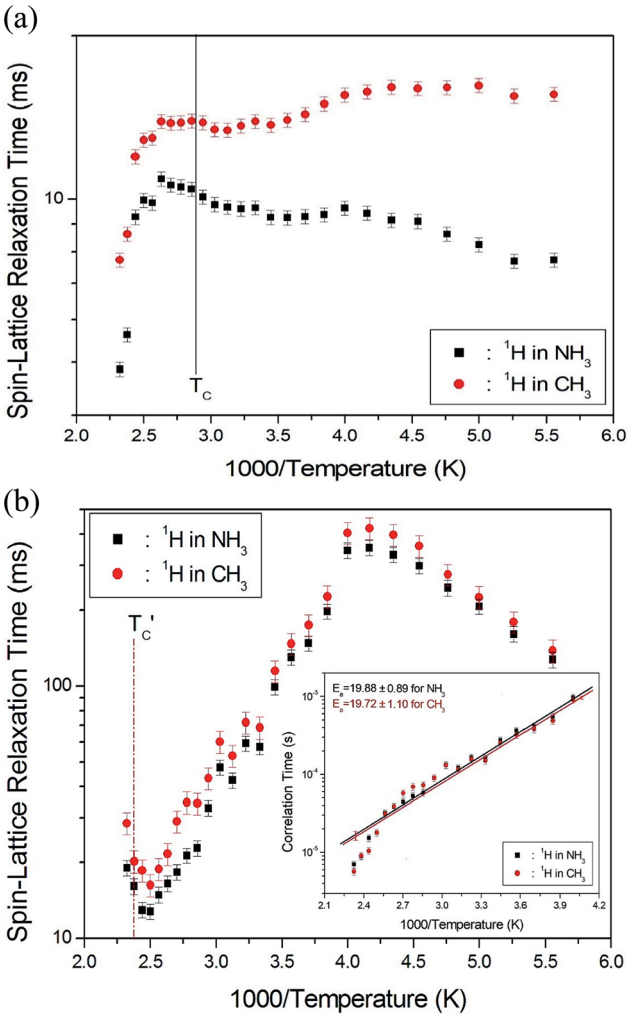

Fig. 5 (a) ^{1}H spin–lattice relaxation times in the rotating coordinate frame for CH_3 and NH_3 groups in $(CH_3NH_3)_2CuCl_4$ as a function of inverse temperature. (b) ^{1}H spin–lattice relaxation times in the rotating coordinate frame for CH_3 and NH_3 groups in $(CH_3NH_3)_2ZnCl_4$ as a function of inverse temperature (inset: Arrhenius plots of the natural logarithm of the correlation time for each proton of CH_3 and NH_3 in $(CH_3NH_3)_2ZnCl_4$ as a function of inverse temperature).

where $a = \tau_C/[1 + \omega_1{}^2\tau_C{}^2]$, $b = \tau_C/[1 + (\omega_H - \omega_C)^2\tau_C{}^2]$, $c = \tau_C/[1 + \omega_C{}^2\tau_C{}^2]$, $d = \tau_C/[1 + (\omega_H + \omega_C)^2\tau_C{}^2]$, and $e = \tau_C/[1 + \omega_H{}^2\tau_C{}^2]$. Here, μ_o is the permeability constant, γ_H and γ_C are the gyromagnetic ratios for the ^{1}H and ^{13}C nuclei, respectively, n is the number of directly bound protons, r is the H–C internuclear distance, $\hbar = h/2\pi$ (where h is Planck's constant), ω_H and ω_C are the Larmor frequencies of ^{1}H and ^{13}C, respectively, and ω_1 is the spin-lock field of 55.55 kHz. Our data are analyzed assuming $T_{1\rho}$ shows a minimum when $\omega_C\tau_C = 1$ and the BPP relation between $T_{1\rho}$ and ω_1 is applicable. As the $T_{1\rho}$ curves are found to exhibit minima, it was possible to determine the coefficient, $0.05(\mu_o/4\pi)^2$ $(\gamma_H\gamma_C\hbar/r_{H-C}{}^3)^2$, in the BPP formula. With this coefficient determined, we were then able to calculate the parameter τ_C as a function of temperature. The temperature dependence of τ_C follows a simple Arrhenius expression, $\tau_C = \tau_{Co}\exp(-E_a/RT)$, where τ_{Co} is the pre-exponential factor, T is the temperature, R is the gas constant, and E_a is the activation energy. Thus, the slope of the straight-line portion of the semi-log plot can be used to determine E_a. The activation energy for the uniaxial rotation of CH_3 and NH_3, obtained from the log τ_C *vs.* $1000/T$ curve shown in the inset of Fig. 5(b), is 19.72 ± 1.10 and 19.88 ± 0.89 kJ mol^{-1}, respectively, and is the same within the error range. In addition, the E_a value for CH_3 and NH_3 at temperatures below 200 K is 6.59 ± 0.51 and 5.92 ± 0.40 kJ mol^{-1}, respectively.

The chemical shifts for ^{13}C in $(CH_3NH_3)_2CuCl_4$ were measured as a function of temperature, as shown in Fig. 6. At room temperature, the ^{13}C CP MAS NMR spectrum shows a signal at a chemical shift of $\delta = 190.50$ with respect to TMS. The ^{13}C chemical shift slowly and monotonously decreases with temperature. In contrast, the chemical shifts for ^{13}C in $(CH_3NH_3)_2ZnCl_4$ were also measured over the temperature range of 180 to 430 K, as shown in the inset of Fig. 6. At room temperature, the ^{13}C CP MAS NMR spectrum possesses two signals at chemical shifts of $\delta = 27.82$ and 29.02. These signals are attributed to the methyl carbons of the two inequivalent sites CH_3 (1) and CH_3 (2), and these results are consistent with the X-ray result previously reported:[18] there exist two kinds of

Open Access Article. Published on 22 May 2018. Downloaded on 4/5/2026 12:25:35 AM.
This article is licensed under a Creative Commons Attribution 3.0 Unported Licence.

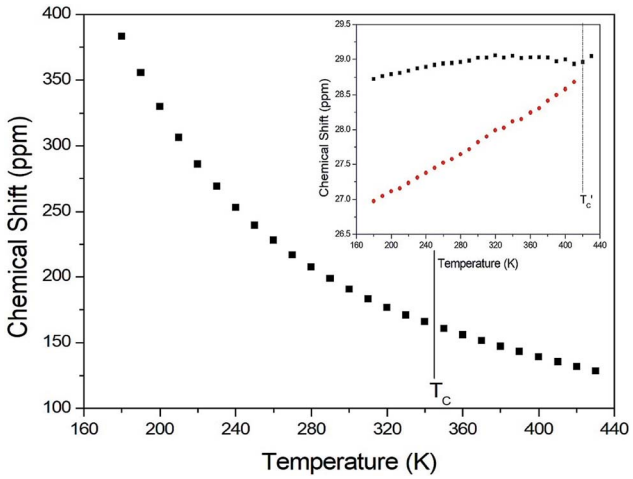

Fig. 6 ^{13}C chemical shift in CH_3 groups in $(CH_3NH_3)_2CuCl_4$ as a function of temperature (inset: that in $(CH_3NH_3)_2ZnCl_4$ as a function of temperature).

crystallographically inequivalent cations. The ^{13}C chemical shifts near 426 K decrease by only one line; the change near 426 K was measured from the ^{13}C chemical shift but not by the DSC result. Although the anomaly was not found around 426 K in the present DSC experiment, the existence of the ^{13}C chemical shift and ^{13}C $T_{1\rho}$ was obtained. This anomaly near 426 K ($= T_C'$) is consistent with that obtained from Raman and IR spectra previously reported. There exist two kinds of inequivalent CH_3 in $(CH_3NH_3)_2ZnCl_4$, whereas only one kind of equivalent CH_3 in $(CH_3NH_3)_2CuCl_4$ exists. On the other hand, the chemical shifts of the CH_3 groups in the ^{13}C NMR spectra were very different between the two compounds. Generally, the paramagnetic contribution to the NMR shift is responsible for the NMR spectra.[40] Thus, the ^{13}C NMR chemical shift of $(CH_3NH_3)_2CuCl_4$, which contain paramagnetic ions, was significantly different from that of $(CH_3NH_3)_2ZnCl_4$, which does not contain paramagnetic ions. The differences in the ^{13}C NMR chemical shifts could potentially be due to differences in the electron structures of the metal ions, in particular, the structure of the d electrons, which screen the nuclear charge from the motion of the outer electrons. Zn^{2+} has a filled d shell, whereas Cu^{2+} has one s electron outside the closed d shell.

The $T_{1\rho}$ values were obtained for the carbon of $(CH_3NH_3)_2MCl_4$ (M = Cu, Zn) at several temperatures. ^{13}C magnetization was generated by CP after spin-locking the protons. All magnetization traces obtained for the methyl carbon were described by a single exponential function $S(t) = S(\infty)\exp(-t/T_{1\rho})$ of eqn (1).[35] The recovery curves for various delay times of ^{13}C in $(CH_3NH_3)_2CuCl_4$ and $(CH_3NH_3)_2ZnCl_4$ were measured at several temperatures. The saturation recovery traces for ^{13}C were measured for delay times ranging from 0.2 to 150 ms at room temperature and are presented in Fig. 7(a) and (b). The recovery traces have different slopes at several temperatures. From these results, the $T_{1\rho}$ values were obtained for the carbon in the two compounds as a function of the inverse temperature. The temperature dependence of the ^{13}C $T_{1\rho}$ values in $(CH_3NH_3)_2CuCl_4$ is illustrated in Fig. 8, and these values are almost constant with temperature. The $T_{1\rho}$ values around T_C are unchanged, in agreement with the conclusion drawn from the ^{13}C chemical shifts. In the case of $(CH_3NH_3)_2ZnCl_4$, the phase transition occurring at T_C' (= 426 K) reported by Perez-Mato *et al.*[23] is not observed from our DSC results, whereas the changes near T_C' are observed by the ^{13}C chemical shift and ^{13}C $T_{1\rho}$ results. Thus, T_C' is denoted by dotted lines in the inset of Fig. 5, 6, and 8. The $T_{1\rho}$ values for the two ^{13}C signals of CH_3 (1) and CH_3 (2) in $(CH_3NH_3)_2ZnCl_4$ are almost the same within the experimental error range.

In order to obtain information concerning the possible distortion surrounding the ^{14}N ion, the NMR spectrum of ^{14}N ($I = 1$) in the laboratory frame was obtained using static NMR at a Larmor frequency of $\omega_0/2\pi = 43.342$ MHz. Two resonance signals were expected from the quadrupole interactions of the ^{14}N nucleus. A magnetic field was applied along the crystallographic axis. The *in situ* ^{14}N NMR spectra and resonance frequency in $(CH_3NH_3)_2ZnCl_4$ single crystals are plotted

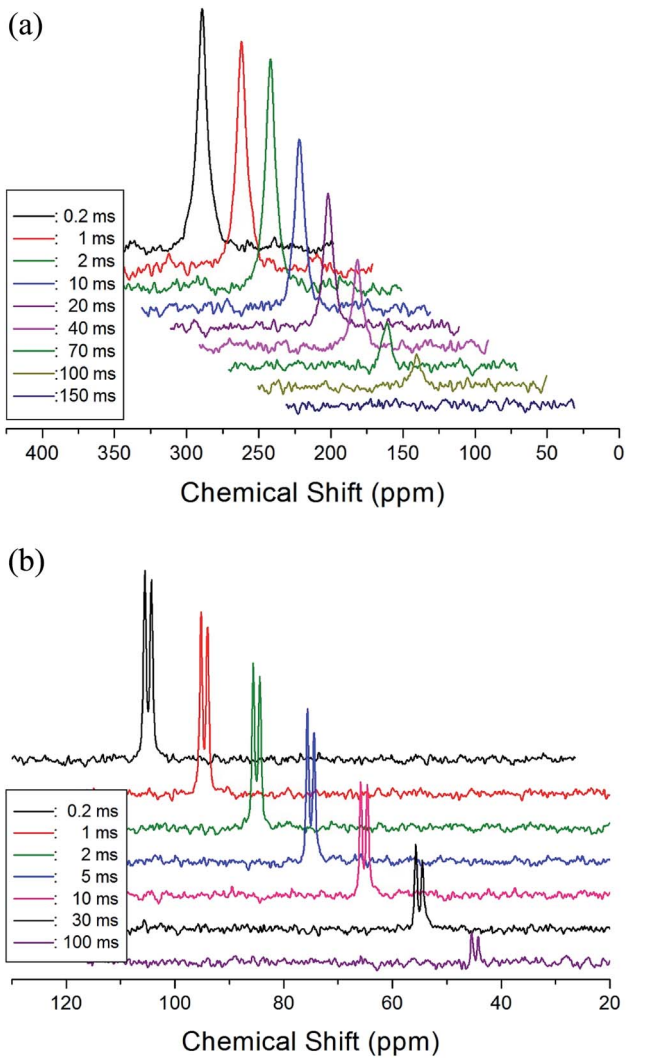

Fig. 7 (a) Recovery spectra for delay times of ^{13}C CP MAS NMR spectrum in $(CH_3NH_3)_2CuCl_4$ at room temperature. (b) Recovery spectra for delay times of ^{13}C CP MAS NMR spectrum in $(CH_3NH_3)_2ZnCl_4$ at room temperature.

This journal is © The Royal Society of Chemistry 2018

Open Access Article. Published on 22 May 2018. Downloaded on 4/5/2026 12:25:35 AM.
This article is licensed under a Creative Commons Attribution 3.0 Unported Licence.

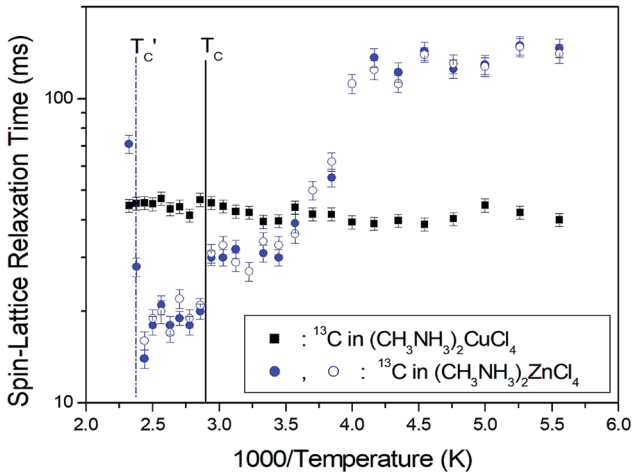

Fig. 8 ^{13}C spin–lattice relaxation times in the rotating coordinate frame for CH_3 groups in $(CH_3NH_3)_2CuCl_4$ and $(CH_3NH_3)_2ZnCl_4$ as a function of temperature.

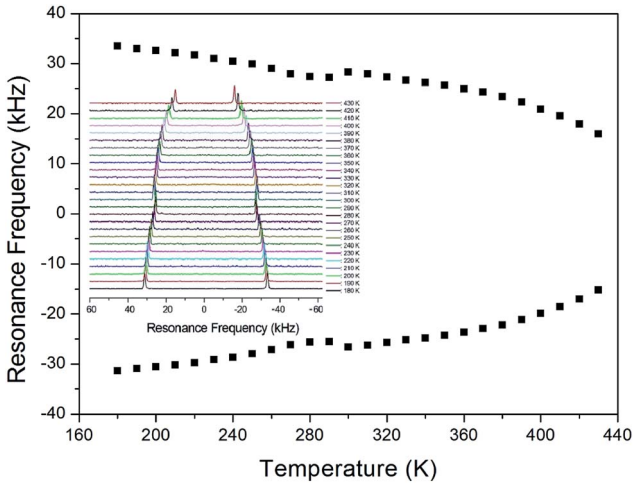

Fig. 9 The temperature-dependent resonance frequency of ^{14}N NMR spectra in $(CH_3NH_3)_2ZnCl_4$ single crystal as a function of temperature (inset: ^{14}N NMR spectra as a function of temperature).

in Fig. 9 as a function of temperature, respectively. The ^{14}N NMR spectra of the two resonance signals for ^{14}N are attributed to the NH_3, and this splitting of the ^{14}N resonance signals slightly decreases with temperature. The small change of the resonance frequency near 300 K is not related to the phase transition. Note that temperature-dependent changes in the ^{14}N resonance frequency are generally attributed to changes in the structural geometry, indicating a change in the quadrupole parameter of the ^{14}N nuclei. The electric field gradient tensors at the N sites vary, reflecting the changing atomic configurations around the nitrogen centers.

4. Conclusions

The ionic dynamics of $(CH_3NH_3)_2MCl_4$ (M = Cu, Zn), focusing on the role of the $CH_3NH_3^+$ cation, were investigated by ^1H MAS NMR, ^{13}C CP MAS NMR, and ^{14}N NMR as a function of temperature. We studied the molecular motions for ^1H and ^{13}C in $(CH_3NH_3)_2MCl_4$ (M = Cu, Zn) based on the spin–lattice relaxation time in the rotating coordinate frame. From the ^1H $T_{1\rho}$ results, we found that the molecular motions for ^1H in $(CH_3NH_3)_2CuCl_4$ are very active at high temperatures. In addition, the activation energies for the uniaxial rotation of ^1H for the CH_3 and NH_3 ions in $(CH_3NH_3)_2ZnCl_4$ have very similar values, and the uniaxial rotation occurs within the high-temperature range. The $T_{1\rho}$ results reveal that the CH_3 and NH_3 cations exhibit high mobility at high temperatures. The $T_{1\rho}$ provides insight into the changes in the cation reorientation rates induced by heating at high temperatures. On the other hand, the minima for $(CH_3NH_3)_2ZnCl_4$ are attributed to the uniaxial rotation of the CH_3NH_3 cations. However, minima such as $T_{1\rho}$ for $(CH_3NH_3)_2CuCl_4$ were not reached for that compound. The lack of a minimum $T_{1\rho}$ indicates that this motion is so slow that there was no detectable $T_{1\rho}$ temperature dependence and also that the uniaxial rotation in $(CH_3NH_3)_2CuCl_4$ was slower than that in $(CH_3NH_3)_2ZnCl_4$. The motion of the CH_3NH_3 cations is slower than the C_3 internal rotation of CH_3 and NH_3; therefore, it reveals $T_{1\rho}$ minima in the high temperature regime above liquid nitrogen temperature. The minima related to the C_3 rotation will appear in the low temperature regime.

A comparison with other compounds of the $(CH_3NH_3)_2MCl_4$ (M = Cu, Zn) indicates a different phase sequence for $(CH_3NH_3)_2MCl_4$ (M = Cd, Mn). For M = Cd, Mn, these systems at room temperature reveal orthorhombic symmetry followed by a tetragonal phase below room temperature. A phase with monoclinic symmetry is also reported at low temperatures. It is interesting to compare the results for $(CH_3NH_3)_2MCl_4$ with those for the analogous compounds containing other metals. In the case of $(CH_3NH_3)_2MnCl_4$ and $(CH_3NH_3)_2CdCl_4$, there is an intermediate tetragonal phase between the monoclinic and orthorhombic phases.[16,31] In contrast, the phase transition sequence for $(CH_3NH_3)_2CuCl_4$ and $(CH_3NH_3)_2ZnCl_4$ changes to an orthorhombic to monoclinic structure with decreasing temperature.[22,31]

The created magnetization decay for each proton in $(CH_3NH_3)_2MCl_4$ (M = Cu, Zn) was analyzed by a single exponential function $S(t)/S(\infty) = A\exp(-t/T_{1\rho})$, whereas that for each proton in $(CH_3NH_3)_2MCl_4$ (M = Mn, Cd) was analyzed by a double-exponential function $S(t)/S(\infty) = A\exp(-t/T_{1\rho}(s)) + B\exp(-t/T_{1\rho}(L))$. These results are consistent with the interactions between the CH_3NH_3 cations and its surrounding MCl_4^{2-} anions. This difference of $T_{1\rho}$ is possibly due to the difference between the electron structures of metal ions. Cu^{2+} and Zn^{2+} have one and two s electrons, respectively, outside the closed d shell; Mn^{2+} has two s electrons in the unfilled 3d orbital; Cd^{2+} has two electrons outside the closed d shell.

The $T_{1\rho}$ values for ^1H of CH_3 and NH_3 indicate that the protons in the CH_3NH_3 cations that are involved in the hydrogen bonding exhibit large and small $T_{1\rho}$ values corresponding to the long C–H and short N–H bonds, respectively. The molecular motion of the cation is induced by heating at high temperatures. The cation dynamics and interionic interactions through hydrogen bonds are expected to be closely related with the physical properties due to the potential

applications. We will be examined the effect for lengths of alkyl chains as further study.

Conflicts of interest

There are no conflicts to declare.

Acknowledgements

This research was supported by the Basic Science Research program through the National Research Foundation of Korea (NRF), funded by the Ministry of Education, Science, and Technology (2016R1A6A1A03012069 and 2015R1A1A3A04001077).

References

1 C. N. R. Rao, A. K. Cheetham and A. Thirumurugan, *J. Phys.: Condens. Matter*, 2008, **20**, 83202.
2 A. H. Arkenbout, T. Uemura, J. Takeya and T. T. M. Palstra, *Appl. Phys. Lett.*, 2009, **95**, 173104.
3 P. Zolfaghari, G. A. de Wijs and R. A. de Groot, *J. Phys.: Condens. Matter*, 2013, **25**, 295502.
4 R. Yadav, D. Swain, P. P. Kundu, H. S. Nair, C. Narayana and S. Elizabeth, *Phys. Chem. Chem. Phys.*, 2015, **17**, 12207.
5 A. M. Elseman, A. E. Shalan, S. Sajid, M. M. Rashad, A. M. Hassan and M. Li, *ACS Appl. Mater. Interfaces*, 2018, **10**, 11699.
6 J. A. Aramburu, P. Garcia-Fernandez, N. R. Mathiesen, J. M. Garcia-Lastra and M. Moreno, *J. Phys. Chem. C*, 2018, **122**, 5071.
7 R. Kind, *Ferroelectrics*, 1980, **24**, 81.
8 A. Rahman, P. R. Clayton and L. A. K. Staveley, *J. Chem. Thermodyn.*, 1981, **13**, 735.
9 A. Levstik, C. Filipic, R. Blinc, H. Arend and R. Kind, *Solid State Commun.*, 1976, **20**, 127.
10 T. Yoshinari, T. Matsuyama, H. Yamaoka and K. Aoyagi, *J. Phys. Soc. Jpn.*, 1989, **58**, 4222.
11 I. R. Jahn, K. Knorr and J. Ihringer, *J. Phys.: Condens. Matter*, 1989, **1**, 6005.
12 H. Manaka, I. Yamada, M. Nishi and T. Goto, *J. Phys. Soc. Jpn.*, 2001, **70**, 1390.
13 A. R. Lim, S. W. Kim and Y. L. Joo, *J. Appl. Phys.*, 2017, **121**, 215501.
14 A. R. Lim, *Solid State Commun.*, 2017, **267**, 18.
15 G. Chapuis, R. Kind and H. Arend, *Phys. Status Solidi A*, 1976, **36**, 285.
16 G. Heger, D. Mullen and K. Knorr, *Phys. Status Solidi A*, 1975, **31**, 455.
17 P. S. R. Prasad, *Phys. Status Solidi A*, 1995, **149**, k13.
18 J. J. M. Steijger, E. Frikkee, L. J. de Jongh and W. J. Huiskamp, *Physica. B*, 1984, **123**, 284.
19 B. Morosin and K. Emerson, *Acta Crystallogr., Sect. B: Struct. Crystallogr. Cryst. Chem.*, 1976, **32**, 294.
20 A. Ben Salah, J. W. Bats, R. Kalus, H. Fuess and A. Daoud, *Z. Anorg. Allg. Chem.*, 1982, **493**, 178.
21 G. Heygster and W. Kleemann, *Physica. B*, 1977, **89**, 165.
22 M. A. White and L. A. K. Staveley, *J. Phys. Chem. Solids*, 1982, **43**, 1019.
23 J. M. Perez-Mato, J. L. Manes, J. Fernandez, J. Zuniga, M. J. Tello, C. Socias and M. A. Arriandiaga, *Phys. Status Solidi A*, 1981, **68**, 29.
24 G. Amirthaganesan, U. Binesh, M. A. Kandhaswamy, M. Dhandapani and V. Srinivasan, *Cryst. Res. Technol.*, 2006, **41**, 708.
25 H. Nishihara, T. Goto, Y. Kimishima and H. Kubo, *J. Phys. Soc. Jpn.*, 1982, **51**, 407.
26 H. Ishida, T. Iwachido, N. Hayama, R. Ikeda, M. Terashima and D. Nakamura, *Zeitschrift für Naturforschung A*, 1989, **44**, 741.
27 H. Kubo, Y. Machida and N. Uryu, *J. Phys. Soc. Jpn.*, 1976, **41**, 1071.
28 H. Kubo, Y. Machida and N. Uryu, *J. Phys. Soc. Jpn.*, 1977, **43**, 459.
29 H. Ishida, *Zeitschrift für Naturforschung A*, 2000, **55**, 412.
30 I. Pabst, J. Karolyi, H. Fuess and M. Couzi, *Phys. Stat. Sol.*, 1996, **155**, 341.
31 I. Pabst, H. Fuess and J. W. Bats, *Acta Crystallogr., Sect. C: Cryst. Struct. Commun.*, 1987, **43**, 413.
32 A. Daoud, *J. Appl. Crystallogr.*, 1977, **10**, 133.
33 R. K. Harris, J. Kowalewski and S. C. de Menezes, *Magn. Reson. Chem.*, 1998, **36**, 145.
34 R. K. Harris, E. D. Becker, S. M. C. de Menezes, R. Goodfellow and P. Granger, *Magn. Reson. Chem.*, 2002, **40**, 489.
35 A. Abragam, *The Principles of Nuclear Magnetism*, Oxford University press, 1961.
36 N. Bloembergen, E. M. Purcell and R. V. Pound, *Phys. Rev.*, 1948, **73**, 679.
37 R. K. Harris, *Nuclear Magnetic Resonance Spectroscopy*, Pitman Pub., UK, 1983.
38 J. L. Koenig, *Spectroscopy of Polymers*, Elsevier, New York, 1999.
39 A. R. Lim, *RSC Adv.*, 2017, **7**, 55276.
40 J. Novotny, M. Sojka, S. Komorovsky, M. Necas and R. Marek, *J. Am. Chem. Soc.*, 2016, **138**, 8432.

Open Access Article. Published on 22 May 2018. Downloaded on 4/5/2026 12:25:35 AM.
This article is licensed under a Creative Commons Attribution 3.0 Unported Licence.

This journal is © The Royal Society of Chemistry 2018